Exchange Boson Dynamics in Cuprates: Optical Conductivity of $HgBa_2CuO_{4+\delta}$

J. Yang,[1,*] J. Hwang,[1,†] E. Schachinger,[2] J. P. Carbotte,[1,5] R. P. S. M. Lobo,[3] D. Colson,[4] A. Forget,[4] and T. Timusk[1,5,‡]

[1]*Department of Physics and Astronomy, McMaster University, Hamilton, ON L8S 4M1, Canada*
[2]*Institute of Theoretical and Computational Physics, Graz University of Technology, A-8010 Graz, Austria*
[3]*Laboratoire Photons et Matière, CNRS UPR5, LPS-ESPCI, 10 rue Vauquelin, 75231 Paris Cedex 5, France*
[4]*CEA, IRAMIS, SPEC, 91191 Gif sur Yvette, France*
[5]*The Canadian Institute of Advanced Research, Toronto, Ontario M5G 1Z8, Canada*
(Received 14 August 2008; published 13 January 2009)

The electron-boson spectral density function $I^2\chi(\Omega)$ responsible for carrier scattering of the high temperature superconductor $HgBa_2CuO_{4+\delta}$ ($T_c = 90$ K) is calculated from new data on the optical scattering rate. A maximum entropy technique is used. Published data on $HgBa_2Ca_2Cu_3O_{8+\delta}$ ($T_c = 130$ K) are also inverted and these new results are put in the context of other known cases. All spectra (with two notable exceptions) show a peak at an energy (Ω_r) proportional to the superconducting transition temperature $\Omega_r \approx 6.3k_BT_c$. This charge channel relationship follows closely the magnetic resonance seen by polarized neutron scattering, $\Omega_r^{\text{neutron}} \approx 5.4k_BT_c$. The amplitudes of both peaks decrease strongly with increasing temperature. In some cases, the peak at Ω_r is weak and the spectrum can have additional maxima and a background extending up to several hundred meV.

Superconductivity arises when electronic quasiparticles bind together into Cooper pairs which condense into a macroscopic quantum state. The interaction which drives the pairing could be charge or spin polarizations, but in conventional metals, it is the polarization of the lattice of ions which provides the necessary attraction. There is also a smaller Coulomb repulsion. In the phonon case Eliashberg theory accounts for all the experimental data with its central ingredient, the electron-phonon spectral density $\alpha^2F(\Omega)$ specifying the boson exchange pairing interaction [1]. Optical spectroscopy is a powerful tool that can be used to extract bosonic spectral density with high degree of accuracy in a variety of systems where other techniques such as tunneling and angle resolved photoemission (ARPES) are difficult to apply. It has been used in conventional metals [2,3] and in the high T_c oxides [4–10] but its interpretation in the cuprates remains controversial. As emphasized recently by Anderson [11], the pairing interaction could involve high energy virtual transitions across the Mott gap with energy set by the Hubbard U which is a large energy and the effective interaction would be instantaneous on the time scale of interest. On the other hand, recent numerical work [12,13] based on the t-J model, has shown that the main contribution to the pairing glue is provided by the spin fluctuations with characteristic energies of at most a few hundred meV. Optical experiments provide a direct probe of this energy region.

The mercury versions of the cuprates, $HgBa_2CuO_{4+\delta}$ (Hg1201) and $HgBa_2Ca_2Cu_3O_{8+\delta}$ (Hg1223) provide a unique opportunity to test these ideas. The one-copper layer system Hg1201 shares a conventional transition temperature around 90 K with widely studied systems YBCO and Bi2212, whereas the three-layer compound Hg1223

has a $T_c = 130$ K, nearly 40% higher. These dramatically different T_c's lead, as we will show, to very different bosonic spectra and place severe constraints on models of superconductivity in the cuprates.

In this Letter, we present new data on the optical constants for $HgBa_2CuO_{4+\delta}$ (Hg1201). The bosonic spectral density $I^2\chi(\Omega)$, recovered by maximum entropy inversion, is found to have a remarkable resemblance to previous results for optimally doped Bi2212 [8]. For further comparison, using the same methods, we also invert published [14] optical constants in the three-layer Hg1223. The high-quality Hg1201 single crystal was grown by a flux growth technique. Our sample was a millimeter sized platelet with a well-oriented ab plane. It is slightly underdoped with a $T_c = 91$ K. The real and imaginary parts of the optical conductivity $\sigma(T, \omega) \equiv \sigma_1(T, \omega) + i\sigma_2(T, \omega)$ follow from the reflectivity. In analyzing optical data, we use a memory function or optical self-energy $\Sigma^{\text{op}}(T, \omega)$ instead of working with $\sigma(T, \omega)$ [15,16]. By definition, $\sigma(T, \omega) = (i\omega_p^2/4\pi)/[\omega - 2\Sigma^{\text{op}}(T, \omega)]$ where ω_p is the plasma frequency. The optical self-energy defined this way plays a role analogous in optics (which involves a two-particle process) to the quasiparticle self-energy $\Sigma^{\text{qp}}(T, \omega)$ in ARPES [17,18]. The optical scattering rate is $1/\tau^{\text{op}}(T, \omega) = -2\Sigma_2^{\text{op}}(T, \omega)$ and the optical effective mass $m^{\text{op}}(T, \omega)/m$ (with m the bare electron mass) is given by $\omega[m^{\text{op}}(T, \omega)/m - 1] \equiv -2\Sigma_1^{\text{op}}(T, \omega)$.

Our results for the real part of the optical self-energy $-2\Sigma_1^{\text{op}}(T, \omega)$, which provides an easy comparison with ARPES, often presented in terms of $2\Sigma_1^{\text{qp}}(T, \omega)$, are shown in Fig. 1 as a function of ω for eight temperatures. The lowest three temperatures are in the superconducting state. The most prominent feature of the curves is the peak
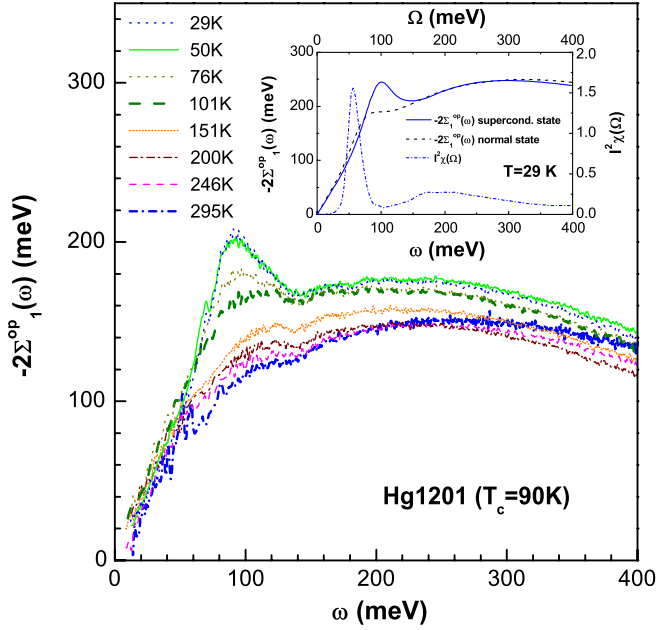
FIG. 1 (color online). Experimental results for the real part of the optical self-energy $-2\Sigma_1^{op}(T, \omega)$ as a function of photon energy ω for eight temperatures. Inset, theoretical results based on numerical solutions of the generalized Eliashberg equations. (Solid blue superconducting and dashed black normal state.) The electron-boson exchange spectral density used is shown as the dash-dotted blue curve. The superconducting gap value is $\Delta = 22.4$ meV.

around 100 meV seen at $T = 29$ K, which progressively disappears as the temperature is increased. To better see how the bosonic spectrum generates the self-energy we show in the inset of the figure a model calculation based on numerical solutions of the d-wave Eliashberg equations. The input electron-boson spectral density $I^2\chi(\Omega)$, shown as the dash-dotted curve, consists of a large narrow peak (right-hand scale) centered at 56 meV followed by a dip and a long background extending beyond 400 meV. The dashed curve, with the same bosonic spectrum, is the normal state result for $-2\Sigma_1^{op}(T, \omega)$ which is to be compared with the solid curve in the superconducting state. The superconducting gap obtained was 22.4 meV giving a gap to T_c ratio, $2\Delta/k_BT_c = 5.8$. Note that, as theory predicts [19], the dashed curve in the normal state shows no visible structure at $\omega = \Omega_r = 56$ meV. Instead there should be zero slope at $\omega = \sqrt{2}\Omega_r$ for an Einstein spectrum. It is clear that boson structure is hard to see in normal state. However, in the superconducting states the quasiparticle electronic density of states acquires energy dependence and this helps reveal the underlying boson structure as seen in the solid blue curve. The peak at ~ 100 meV is neither at Ω_r nor $\sqrt{2}\Omega_r$ but is shifted upwards by the opening of the gap Δ [19] but as we see, the position of the peak in $I^2\chi(\Omega)$ cannot be read off the curve without the knowledge of the value of the superconducting gap.

In Fig. 2(b) we show results for the spectral density $I^2\chi(\Omega)$ of maximum entropy inversions augmented with a least squares improvement based on the full d-wave Eliashberg equations [6]. Further applications are found in Refs. [8–10]. The input to the inversion is the optical scattering rate $1/\tau(\omega) = \frac{\omega_p^2}{4\pi} \text{Re}[1/\sigma(\omega)]$. These are shown in Fig. 2(a) where the results of our inversions (heavy lines) are compared with the original data (light lines). In all cases, the fit is very good. Recently, van Heumen *et al.* [20,21] have also presented optical data for Hg1201 above T_c which they analyze in terms of a spectral density represented by a set of histograms. While they obtain fits which are of equal quality to ours and have a background extending to >400 meV as we have, they find that the height of the peak at 56 meV does not change contrary to our findings for $T = 246$ and 295 K. This has been taken as evidence for coupling of the charge carriers to phonons [22]. We can also get fits where the peak height does not
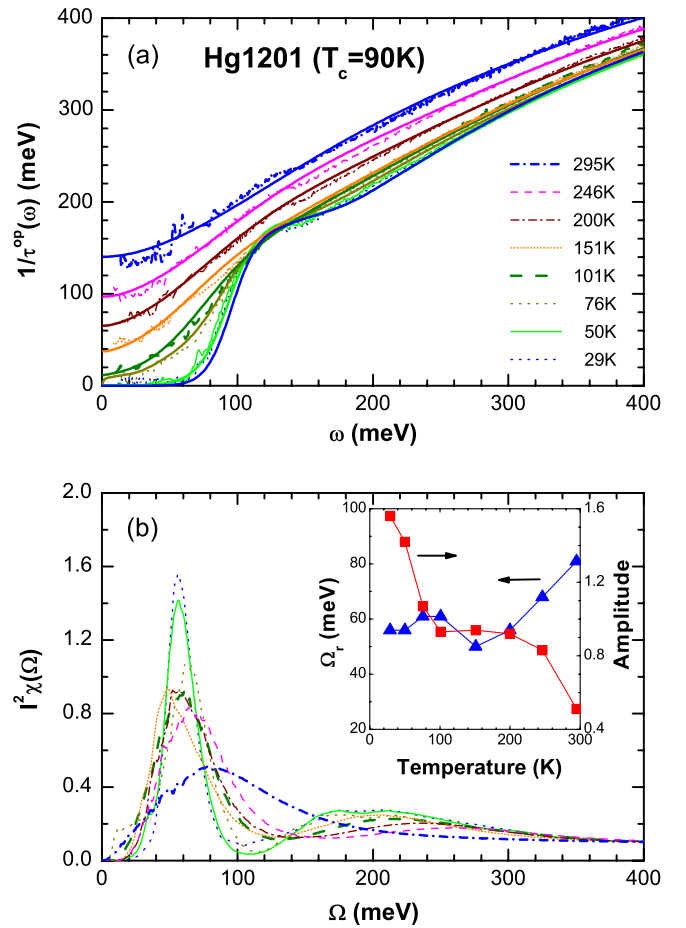
FIG. 2 (color online). Top frame, the optical scattering rate $1/\tau^{op}(T, \omega)$ for Hg1201 vs ω for 8 temperatures (light curves). The wider curves are our maximum entropy reconstructions. Bottom frame, the electron-boson spectral function $I^2\chi(\Omega)$ vs Ω. The inset gives the peak position (blue triangles) left scales as a function of temperature and the red squares give the corresponding peak amplitude.

change but only if we use a *biased* maximum entropy inversion with the default model set to the previous lower temperature solution instead of being set to the constant of the *unbiased* inversion.

In the inset to the lower frame of Fig. 2, we show the frequency (left scale, triangles) of the prominent peak in $I^2\chi(\Omega)$ as a function of temperature. As also noted by van Heumen *et al.* [20], Ω_r is fairly constant at ~56 meV but in our analysis, this frequency clearly increases for T above 200 K. More importantly, the amplitude of the peak shows strong temperature dependence in the superconducting state and also above 200 K. Further, the width of the peak increases with increasing T. As noted for Bi2212 [8], the shift in spectral weight into the peak at 60 meV can be interpreted to proceed through a transfer of spectral weight from high to low frequencies as the temperatures is lowered. We note here that in contrast a bosonic function from the electron-phonon interaction would not have these properties: its amplitude, width, and center frequency would all be temperature independent and would not vary from one cuprate to another (as shown in Fig. 4 below).

In Fig. 3 we display similar results for Hg1223 with $T_c = 130$ K. In Fig. 3(a) we reproduce the optical scattering rate at four temperatures (with $T = 15$ and 125 K in the superconducting state) from the work of McGuire *et al.* [14]. Our results for $I^2\chi(\Omega)$ are presented in Fig. 3(b) and the quality of the data reconstruction is demonstrated by the heavy lines in Fig. 3(a) to be compared with the corresponding light line (data). We find significant residual (static impurity $1/\tau_{\mathrm{imp}} \simeq 95$ meV) scattering rate in contrast to Hg1201 which is in the clean limit ($1/\tau_{\mathrm{imp}} = 0$). The superconducting state data (blue, dotted curve) for $1/\tau^{\mathrm{op}}(\omega)$ at $T = 15$ K shows a peak around 140 meV which is the indication of a gap in the charge carrier density of states (DOS). Currently there is no known kernel which allows maximum entropy inversion of such data and so we do not show results in this instance. On the other hand, in the $T = 125$ K data there is no signature of such a DOS gap. Results are shown in Fig. 3(b). The prominent peak at $\Omega_r \cong 72$ meV seen in the curve at $T = 125$ K is missing at higher T. In contrast to the Hg1201 case no reasonable alternate fits can be found for $T = 225$ and 295 K which show a significant peak amplitude at 72 meV.

In Fig. 4, we place our results for Ω_r, the frequency of the peak in $I^2\chi(\Omega)$, in the context of other such results by plotting Ω_r as a function of the superconducting T_c for a number of cuprates. In all cases, $I^2\chi(\Omega)$ has been extracted from the optical data but not always using a maximum entropy technique. Some are fits to assumed forms including a broad background introduced in Ref. [23] to model antiferromagnetic fluctuations, augmented with a resonance peak. Both methods give very much the same results as documented in Ref. [5]. The heavy long dashed line is a least square fit to all the optical data and gives $\Omega_r \approx$
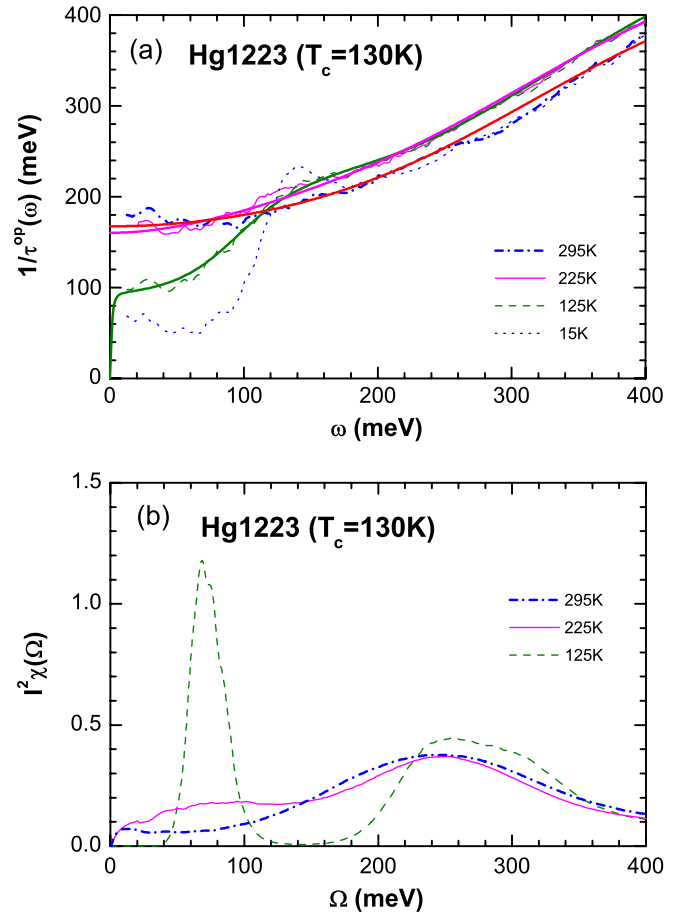
FIG. 3 (color online). Same as Fig. 2 but for Hg1223 ($T_c = 130$ K).

$6.3k_BT_c$. This is close to, but not quite, the position of the spin-one neutron resonance obtained by He *et al.* [24,25] where $\Omega_r^{\mathrm{neutron}} \approx 5.4k_BT_c$ represented in Fig. 4 as the dotted line.

Several comments should be made about such a comparison between charge excitations and the magnetic susceptibility. First, the neutron resonance plotted in Fig. 4 refers to the sharp peak that appears at $q = (\pi, \pi)$ whereas the bosonic function that governs the optical response is the q averaged local susceptibility. This arises because the Fermi-surface to Fermi-surface electron scattering involves momentum transfers to boson excitations that span all momenta in the Brillouin zone, some involving umklapp processes. Where magnetic neutron scattering data for the q-averaged susceptibility are available such as the Ortho II YBCO [26] or optimally doped LSCO [27] the agreement between the neutron data and the optical data is excellent: not only are the peaks in the response at the same frequencies but also the temperature dependence of the amplitude of the peaks are in agreement [8,9]. Second, it should be noted that in some cuprates, the resonance described involves only a very small fraction of the total weight seen in the local spin susceptibility as in
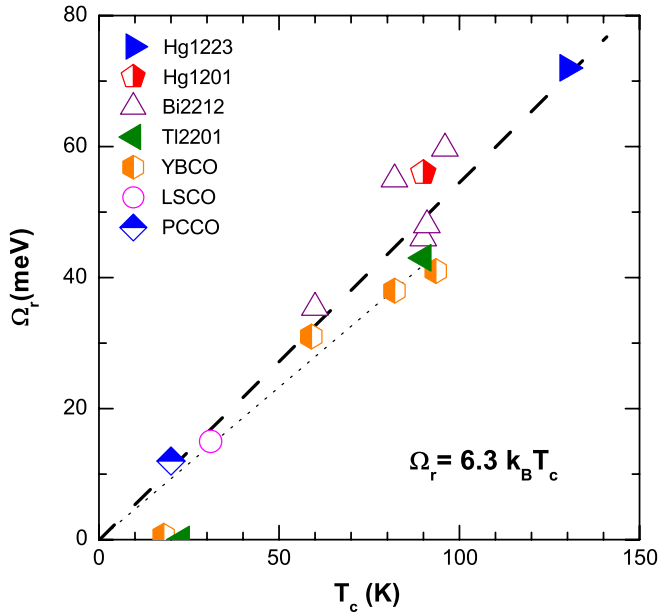
FIG. 4 (color online). The optical resonance frequency Ω_r as a function of T_c. Bi2212 [6,8], Tl2201 [5], YBCO [5–7], LSCO [9], and PCCO [10].

Note added in proof.—We have learned of a neutron scattering study by Yu *et al.* [31], where a magnetic resonance in optimally doped Hg1201 is reported at 56 meV, exactly the same energy as the peak we found here. Recent Raman data find a superconducting gap 2Δ very close to the values found in our calculations [32].

LaSrCuO [9] and PrCeCuO [10]. In $YBCO_{6.5}$ it is estimated to be 3% [26] and in some cases there is no resonance [5,28], but it is always the local, Brillouin zone averaged spin susceptibility which controls superconductivity. Finally, the two points at $\Omega_r = 0$ (not used in the fit to the data in Fig. 4) are for $YBCO_{6.35}$ [28] and overdoped Tl2201 [5]. In both cases, no optical resonance could be identified. The resonance may enhance but is not essential for superconductivity in the cuprates and the scaling of the position of the peak with T_c shown in Fig. 4 must be the result and not the cause of the rearrangement of the electronic DOS in the superconducting state as suggested by several theorists [29,30]. We also note here that recent dynamical mean field calculations of the one-band Hubbard model yield bosonic spectral functions very similar to what is shown in Figs. 2 and 3 [12,13].

In summary we find that in Hg1201 and Hg1223 optical resonances are found in maximum entropy inversions of the optical scattering, at 56 and 72 meV, respectively. However, when the temperature is increased towards 300 K, the spectral weight under this resonance moves to higher energy and broadens significantly, in contrast to the findings of van Heumen *et al.* [21]. The optical resonance scales with T_c over a broad set of materials with $\Omega_r \approx 6.3k_BT_c$ which is remarkably close to the energy of the spin-one resonance seen in polarized neutron scattering, namely $\Omega^{\mathrm{neutron}} = 5.4k_BT_c$ leaving no doubt that the charge carriers are coupled to spin fluctuations, while there is no evidence for an important phonon contribution.

*Current address: School of Materials Science and Engineering, Tianjin University, Tianjin 300072, People's Republic of China.
†Present address: Department of Physics, University of Florida, Gainesville, FL 32611, USA.
‡timusk@mcmaster.ca
[1] J. P. Carbotte, Rev. Mod. Phys. **62**, 1027 (1990).
[2] B. Farnworth and T. Timusk, Phys. Rev. B **10**, 2799 (1974).
[3] F. Marsiglio *et al.*, Phys. Lett. A **245**, 172 (1998).
[4] J. P. Carbotte *et al.*, Nature (London) **401**, 354 (1999).
[5] E. Schachinger and J. P. Carbotte, Phys. Rev. B **62**, 9054 (2000).
[6] E. Schachinger *et al.*, Phys. Rev. B **73**, 184507 (2006).
[7] J. Hwang *et al.*, Phys. Rev. B **73**, 014508 (2006).
[8] J. Hwang *et al.*, Phys. Rev. B **75**, 144508 (2007).
[9] J. Hwang *et al.*, Phys. Rev. Lett. **100**, 137005 (2008).
[10] E. Schachinger *et al.*, Phys. Rev. B **78**, 134522 (2008).
[11] P. W. Anderson, Science **316**, 1705 (2007).
[12] T. A. Maier *et al.*, Phys. Rev. Lett. **100**, 237001 (2008).
[13] B. Kyung *et al.*, arXiv:0812.1228.
[14] J. J. McGuire *et al.*, Phys. Rev. B **62**, 8711 (2000).
[15] A. V. Puchkov *et al.*, J. Phys. Condens. Matter **8**, 10 049 (1996).
[16] T. Mori *et al.*, Phys. Rev. B **77**, 174515 (2008).
[17] P. D. Johnson *et al.*, Phys. Rev. Lett. **87**, 177007 (2001).
[18] J. Hwang *et al.*, Phys. Rev. Lett. **98**, 207002 (2007).
[19] J. P. Carbotte *et al.*, Phys. Rev. B **71**, 054506 (2005).
[20] E. van Heumen *et al.*, arXiv:0807.1730 (unpublished).
[21] E. van Heumen *et al.*, Phys. Rev. B **75**, 054522 (2007).
[22] J. Lee *et al.*, Nature (London) **442**, 546 (2006).
[23] A. J. Millis *et al.*, Phys. Rev. B **42**, 167 (1990).
[24] H. He *et al.*, Phys. Rev. Lett. **86**, 1610 (2001).
[25] H. He *et al.*, Science **295**, 1045 (2002).
[26] C. Stock *et al.*, Phys. Rev. B **71**, 024522 (2005).
[27] B. Vignolle *et al.*, Nature Phys. **3**, 163 (2007).
[28] C. Stock *et al.*, Phys. Rev. B **73**, 100504(R) (2006).
[29] Ar. Abanov and A. V. Chubukov, Phys. Rev. Lett. **83**, 1652 (1999).
[30] P. Prelovšek and I. Sega, Phys. Rev. B **74**, 214501 (2006).
[31] G. Yu *et al.*, arXiv:0810:5759.
[32] W. Guyard *et al.*, Phys. Rev. Lett. **101**, 097003 (2008).